Structure and Binding for Complexes of Rebek's Acridine Diacid with Pyrazine, Quinoxaline, and Pyridine from Monte Carlo Simulations with an All-Atom Force Field

Erin M. Duffy and William L. Jorgensen*

Contribution from the Department of Chemistry, Yale University, New Haven, Connecticut 06511

Received March 11, 1994[®]

Abstract: The structures and relative binding free energies for complexes of pyrazine and pyridine with Rebek's acridine diacid in chloroform have been revisited through Monte Carlo statistical mechanics calculations at 25 °C. In order to further probe the reported selectivity of the host and to clarify the nature of binding benzo derivatives of pyrazine, computations were also carried out for quinoxaline. The calculations feature advances to a fully flexible all-atom model for the host. The guests, also represented by all-atom potential functions, were gradually mutated into one another both bound to the diacid and unbound in solution. Statistical perturbation theory (SPT) afforded the associated free energy changes, which combine to yield the relative free energies of binding. The experimentally observed binding order, quinoxaline > pyrazine > pyridine, was reproduced, and structures supporting two-point binding for the diazine guests were found. Energetic and structural comparisons with the earlier computational study are made, and the origin of the modest difference in binding pyrazine over pyridine is analyzed. An explanation for the enhanced binding of quinoxaline that does not include π-stacking with the acridine spacer is provided, and the computed structures are compared with those hypothesized by Rebek as well as those recently published by Pascal and Ho.

Introduction

Rebek and co-workers have demonstrated the utility of cleft-shaped molecules for binding neutral guests through hydrogen bonding.[1] The inward-directed functionality is reminiscent of the disposition of reactive side chains in enzyme active sites and provides an attractive framework for the development of synthetic catalysts.[1] A prototypical example is provided by the complex **1** between pyrazine and the acridine diacid host. On the basis

1
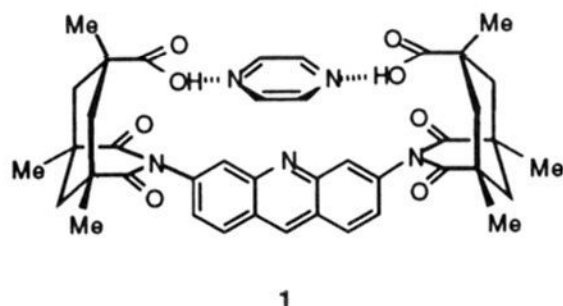
of binding and NMR chemical shift data for diazine and diamine guests such as pyrazine and diazabicyclobutane (DABCO), the two-point hydrogen bonding as in **1** was proposed for the complexes in chloroform.[2] However, subsequent Monte Carlo simulations for **1** indicated that the cleft was too small for simultaneous two-point binding.[3] Pyrazine was found to lie above the plane of the acid groups with one well-formed hydrogen bond and a weaker electrostatic attraction between the second acid group and nitrogen.[3] This seemed to account for the relatively small preference for binding pyrazine over pyridine, a factor of 12 in K_a (1.5 kcal/mol), which was reproduced well by the free energy calculations.[3]
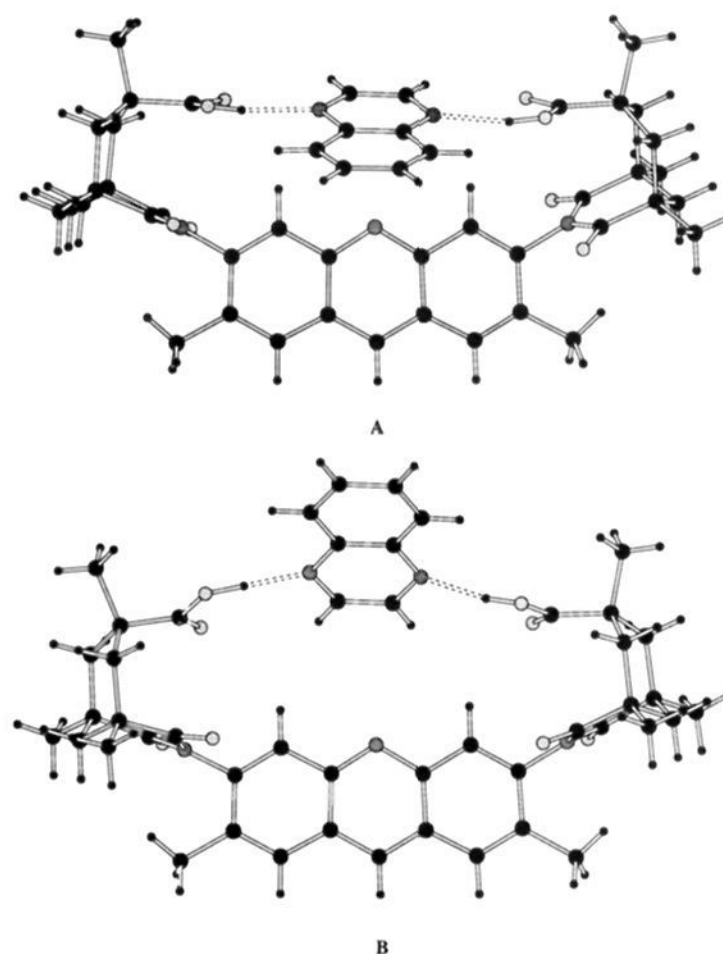
The structural issue is a central one for the design, elaboration, and modeling of such complexes. Important additional data have

Figure 1. X-ray structures of Rebek's diacid–quinoxaline complexes A (top) and B (bottom) from ref 4.

recently been provided through a crystal structure for the complex of the acridine diacid with quinoxaline.[4] The two crystallographically independent forms of the complex in the asymmetric unit are illustrated as A and B in Figure 1. Both exhibit nearly symmetrical two-point binding. In complex A, the O_H–O_H distance is 8.36 Å and the two hydrogen bonds are approximately linear. In B, the smaller O_H–O_H separation, 7.93 Å, is accompanied by bent hydrogen bonding, with the quinoxaline nitrogens about 0.7 Å above the plane of the carbonyl oxygens. In chloroform solution, quinoxaline is more tightly bound than

[®] Abstract published in *Advance ACS Abstracts*, June 1, 1994.

(1) (a) Rebek, J., Jr. *Science* **1987**, *235*, 1478. (b) Rebek, J., Jr. *Acc. Chem. Res.* **1990**, *23*, 399 and references therein. (c) Rebek, J., Jr.; Marshall, L.; Wolak, R.; Parris, K.; Killoran, M.; Askew, B.; Nemeth, D.; Islam, N. *J. Am. Chem. Soc.* **1985**, *107*, 7476.

(2) (a) Rebek, J., Jr.; Nemeth, D. *J. Am. Chem. Soc.* **1986**, *108*, 5637. (b) Rebek, J., Jr.; Askew, B.; Killoran, M.; Nemeth, D.; Lin, F.-T. *J. Am. Chem. Soc.* **1987**, *109*, 2426.

(3) Jorgensen, W. L.; Boudon, S.; Nguyen, T. B. *J. Am. Chem. Soc.* **1989**, *111*, 755.
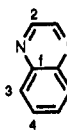
(4) Pascal, R. A., Jr.; Ho, D. M. *J. Am. Chem. Soc.* **1993**, *115*, 8507.

Table 1. Computed 6-31G(d) Atomic Charges for Guest Molecules

molecule	atom	q (Mulliken)	q (CHELPG)
	N	−0.4634	−0.4618
	C	+0.0150	+0.1832
	H	+0.2167	+0.0477
	N	−0.5177	−0.6697
	C1	+0.0641	+0.4609
	C2	−0.2547	−0.4488
	C3	−0.1442	+0.2328
	H1	+0.2030	+0.0177
	H2	+0.2110	+0.1561
	H3	+0.2151	+0.0651
	N	−0.531	−0.538
	Cf	+0.236	+0.377
	C2	+0.035	+0.187
	C3	−0.166	−0.302
	C4	−0.180	−0.098
	H2	+0.205	+0.065
	H3	+0.206	+0.177
	H4	+0.195	+0.132

pyrazine by a factor of 16 in K_a at 25 °C (1.6 kcal/mol).[2] The enhancement was proposed to result from π-stacking of the benzenoid ring of the quinoxaline and the acridine fragment;[2] however, this interaction is not found in structures A and B.

Furthermore, a crystal structure for the complex with pyrazine (1) has now been obtained and shows two-point binding.[5] The origin of the small difference in binding pyrazine over pyridine again becomes puzzling, though it has been suggested that some strain may be introduced in achieving the two-point binding geometry for the host.[4] The discrepancy with the computed structure for 1 also needs clarification; if the computed structures are in error, the reasonable calculated results for the pyrazine/ pyridine K_a ratio are fortuitous.[3] This is possible since the calculations only sampled six torsional degrees of freedom and no angle bending for the host. This may not have allowed adequate flexibility for the binding cleft to permit two-point binding.[6] Another possibility is that the structures of the complexes are not the same in chloroform at 298 K as they are in the crystalline environment at 235 K.[4,6]

These questions are all addressed in the present computational study, which brings the modeling up to current standards. In particular, an all-atom force field has been used with complete flexibility for the complexes, except within the aromatic rings. The differences in free energy of binding for pyrazine versus both pyridine and quinoxaline in chloroform have been obtained, along with detailed structural results for the complexes. A coherent picture emerges that illuminates the intrinsic structures and energetics for the complexes in the gas phase, the structures for the complexes in chloroform, the origins of the observed differences in binding affinities, the significance of π-stacking interactions, and the discrepancy between the prior structure computed for 1 and the crystallographic results.

Computational Details

Force Field. The intermolecular and intramolecular interactions were described by the AMBER/OPLS force field.[7–9] In order to model accurately the flexibility in the acridine diacid host, an all-atom representation was used. The requisite nonbonded parameters for the host were adapted from established OPLS potentials, which consist of Coulombic and Lennard–Jones terms. In particular, the acridine spacer was a composite of arene and nucleotide base parameters, and the bicyclic

pieces were based on hydrocarbon, carboxylic acid, and simple peptide fragments.[9–13] Intramolecular 1,4 nonbonded interactions were included with a scaling factor of 2 for both the electrostatic and Lennard–Jones terms.[9]

The energetics of bond stretching and angle bending in the host were based on the AMBER force field using quadratic terms.[7] All torisonal degrees of freedom were also sampled except within the aromatic rings. The energetics of such motions were described by OPLS and OPLS93 torsional parameters.[9,12] These have been obtained primarily by fitting to torsional energy profiles from ab initio 6-31G(d)//6-31G(d) calculations on small organic molecules representative of peptide fragments.[9] The total intramolecular potential energy consists of the torsional contribution given by a Fourier series (eq 1) plus the intramolecular bond

$$V(\phi) = V_0 + {}^1/_2 V_1[1 + \cos(\phi + f_1)] +$$
$$ {}^1/_2 V_2[1 - \cos(2\phi + f_2)] + {}^1/_2 V_3[1 + \cos(3\phi + f_3)] \quad (1)$$

stretching, angle bending, and nonbonded interactions. The latter terms are backed out of the total energy to derive the Fourier coefficients for the remaining energy contributions from eq 1. For the present purposes, additional torsional parameters were needed for the pivalic acid-like fragments of the host. These were obtained in an analogous manner using MM3 results obtained from MacroModel[14] for the torsional profiles about the C_α–C bond in pivalic acid and the C–O(H) bond in acetic acid.

The guests, pyridine, pyrazine, and quinoxaline, were treated as rigid molecules, i.e., they only contribute to the total energy through nonbonded interactions with the host and solvent molecules. Because the necessary partial charges were not available, single point ab initio 6-31G(d) calculations were carried out with GAUSSIAN 92[15] for each monomer at its experimental geometry.[5,16] This generated Mulliken charges from a standard population analysis and CHELPG charges from a fit to the electrostatic potential surface of each guest (Table 1).[17] Given that the 6-31G(d) CHELPG charges have been shown to be far superior to the Mulliken charges in reproducing experimental free energies of hydration for organic molecules,[18] the CHELPG charges were used for the present calculations, though some results are also reported with the Mulliken charges for comparison. The Lennard–Jones interactions were modeled with standard OPLS parameters for nucleotide bases coupled with, in the case of quinoxaline, standard arene values.[10,11] It may be noted that in the prior study[18] the use of 6-31G(d) CHELPG charges and OPLS Lennard–Jones parameters led to a computed free energy of hydration for pyridine in exact agreement with the experimental value.

For the binding calculations in chloroform, the OPLS four-site model was used for the solvent molecules with the hydrogen implicit.[8]

A complete listing of the force field parameters used for the host–guest systems is provided as supplementary material.

Monte Carlo Simulations. Relative free energies of binding ($\Delta\Delta G$) for pyrazine versus pyridine as well as quinoxaline versus pyrazine with the acridine diacid in chloroform were computed through the following thermodynamic cycle
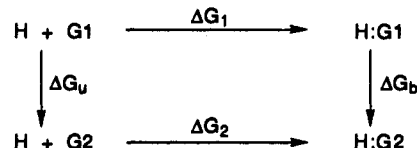
where the experimentally measured relative binding free energy, ΔG_2 − ΔG_1, is equivalent to the computationally procured ΔG_b − ΔG_u.[19] The latter free energy changes were afforded by Metropolis Monte Carlo (MC) simulations using statistical perturbation theory (SPT).[20,21] The relative binding constants, moreover, were readily computed from these $\Delta\Delta G$'s via $K_{rel} = \exp(-\Delta\Delta G/RT)$.

In practice, employment of the thermodynamic cycle to obtain one relative binding free energy involved two sets of mutations. The first leg
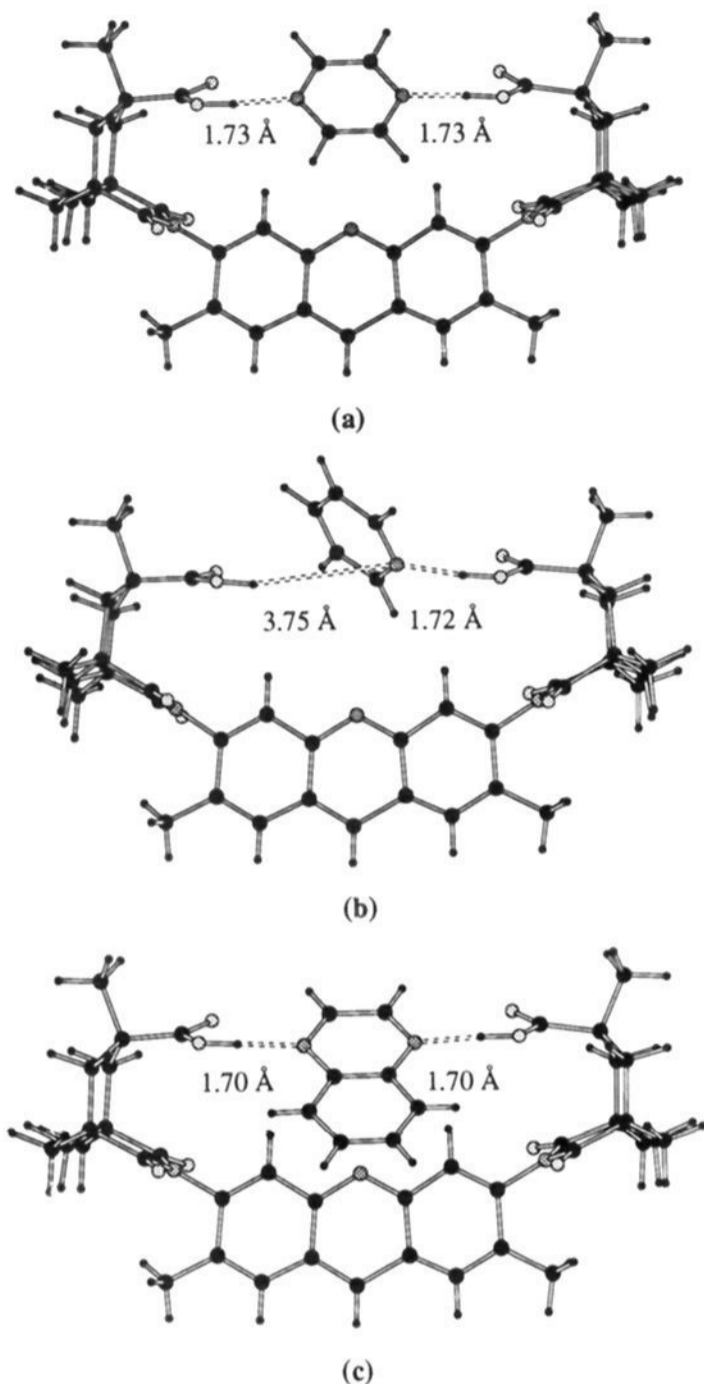
(5) Pascal, R. A., Jr.; Ho, D. M. To be published.

(6) Jorgensen, W. L.; Duffy, E. M. *Chemtracts: Org. Chem.* **1994**, *6*, 300.

(7) (a) Weiner, S. J.; Kollman, P. A.; Case, D. A.; Singh, U. C.; Ghio, C.; Alagona, G.; Profeta, S.; Weiner, P. *J. Am. Chem. Soc.* **1984**, *106*, 765. (b) Weiner, S. J.; Kollman, P. A.; Nguyen, D. T.; Case, D. A. *J. Comput. Chem.* **1986**, *7*, 230.

(8) Jorgensen, W. L.; Tirado-Rives, J. *J. Am. Chem. Soc.* **1988**, *110*, 1657.

(9) Maxwell, D. S.; Tirado-Rives, J.; Jorgensen, W. L. *J. Comput. Chem.* **1994**, *15*, in press.

(10) Jorgensen, W. L.; Severance, D. L. *J. Am. Chem. Soc.* **1990**, *112*, 4768.

(11) Pranata, J.; Wierschke, S. G.; Jorgensen, W. L. *J. Am. Chem. Soc.* **1991**, *113*, 2810.

(12) (a) Jorgensen, W. L.; Severance, D. L. *J. Am. Chem. Soc.* **1991**, *113*, 209. (b) Kaminski, G.; Duffy, E. M.; Matsui, T.; Jorgensen, W. L. *J. Am. Chem. Soc.* **1994**, *116*, in press.

(13) Briggs, J. M.; Nguyen, T. B.; Jorgensen, W. L. *J. Phys. Chem.* **1991**, *95*, 3315.

(14) Still, W. C. *MacroModel*, Version 3.5a; Columbia University: New York, 1992.

(a)

(b)

(c)

Figure 2. Gas-phase energy minima for the acridine diacid host with (a) pyrazine, (b) pyridine, and (c) quinoxaline. Acid–nitrogen hydrogen bonds are dashed.

entailed gradual mutation of the geometrical and energetic parameters of one guest (pyrazine or quinoxaline) to those of the other (pyridine or pyrazine) bound to the diacid, yielding ΔG_b. The guests were then interconverted by themselves in chloroform to give ΔG_u in the "free" or unbound mutations. This methodology and its application to numerous organic host–guest systems have been described previously.[21,22]

For all the components of the system, initial geometries were based on X-ray crystallographic data.[4,5,16,23,24] Owing to the fact that a structure for quinoxaline was not available, the coordinates were taken from the quinoxaline in the acridine diacid complex, for which a high-resolution structure was recently obtained.[4]

Initially, the acridine diacid was subjected to a regime of gas-phase optimizations with the BOSS program,[25] where the convergence criterion for the Fletcher–Powell method was specified as 1×10^{-4} kcal/mol. In order to gain some information about the binding interactions, optimiza-

Table 2. Breakdown of Gas-Phase Net Interaction Energies (kcal/mol) for Complexes[a]

complex	ΔE	ΔE deformation	E_{XX}	$1/r$	$1/r^{12}$	$1/r^6$
pyrazine	−17.17	3.43	−20.60	−17.38	15.24	−18.46
pyridine	−13.84	1.85	−15.69	−11.13	10.51	−15.07
quinoxaline	−23.26	3.46	−26.72	−20.17	19.67	−26.22

[a] ΔE is the net interaction energy consisting of the energy difference between the bound and unbound host (ΔE deformation) and the host–guest interaction (E_{XX}). E_{XX} is further broken down into its Coulombic ($1/r$) and Lennard–Jones ($1/r^{12}$ and $1/r^6$) terms.

tions were also carried out for each host–guest pair. It is emphasized that in both the gas-phase optimizations and the Monte Carlo simulations all bond lengths, bond angles, and dihedral angles for the host were varied, except for those of the acridine fragment. Translations and rigid-body rotations for the guests were also performed. For the Monte Carlo calculations, each system comprised the characteristic host–guest pair plus 380 chloroform molecules and occupied periodic cells with dimensions ca. $33 \times 33 \times 49.5$ Å^3. Initially, the acridine diacid was oriented along the long axis of the periodic cell. The solute–solvent and solvent–solvent interactions were truncated at 11 Å and were quadratically feathered to zero over the last 0.5 Å. The cutoff procedure for the solute–solvent interactions involved the distances of the carbon of chloroform to a well-distributed set of atoms in the solute; if any of these was within the cutoff, the solute–solvent interaction was included. In view of the large number of intramolecular degrees of freedom in the host, a solute move was attempted every 15 configurations. The ranges for the variations of the internal degrees of freedom in the host as well as for translations and rotations of the guests and solvent molecules were adjusted to yield new configurations with a ca. 40% acceptance rate.

Calculations on a model host were also performed in order to isolate the interactions among the guests and the acid groups of the Rebek diacid. Two OPLS united-atom acetic acid molecules were oriented as in the acridine diacid crystal, and a series of gas-phase optimizations was performed. First, the pyrazine–diacid and pyridine–diacid complexes were fully optimized, with the cleft size fixed at the optimal geometry for pyrazine. Next, the non-hydrogen-bonded acid group for the pyridine complex was removed, and the monoacid complex was optimized in the interest of understanding the role of the second acid group. Finally, the model pyrazine/pyridine mutation in chloroform was performed, using the same protocol as above.

To probe the sensitivity of the energetics and structures of the complexes to the electrostatic model chosen to represent the guests, the repertoire of simulations was also performed for pyrazine and pyridine, with the Mulliken charges.

In all cases, standard procedures were employed in the isothermal–isobaric (NPT) ensemble at 25 °C and 1 atm. The number of mutation steps (separate simulations) was set at 10 ($\Delta\lambda = 0.050$) for the bound mutations and four ($\Delta\lambda = 0.125$) for the free mutations, and "double-wide" sampling was implemented.[26] The endpoints in each bound mutation, furthermore, were subjected to a straight MC run to study further the structures of the complexes. Each step involved an equilibration phase consisting of 4×10^5 configurations in which only the solutes were allowed to move, 4×10^5 configurations in which only the solvent molecules could move, and 1×10^6 configurations of NPT–MC equilibration. The averaging period of 2×10^6 configurations followed from this structure. The unbound mutations employed a less complicated agendum that included an equilibration phase of 2×10^6 configurations followed by averaging over 4×10^6 configurations. The model mutations were run over five windows ($\Delta\lambda = 0.100$) and according to the same schedule as the unbound mutations. All calculations were performed with the BOSS program[25] on Silicon Graphics 4D/35 and R/4000 computers.

Results and Discussion

Gas-Phase Structures and Energetics. The key results from optimizations of the acridine diacid and its complexes are given in Figure 2a–c and Table 2.

(15) Frisch, M. J.; Trucks, G. W.; Head-Gordon, M.; Gill, P. M. W.; Wong, M. W.; Foresman, J. B.; Johnson, B. G.; Schlegel, H. B.; Robb, M. A.; Replogle, E. S.; Gomperts, R.; Andres, J. L.; Raghavashari, K.; Binkley, J. S.; Gonzalez, C.; Martin, R. L.; Fox, D. L.; Defrees, D. J.; Baker, J.; Stewart, J. J. P.; Pople, J. A. *GAUSSIAN 92*, Revision E.2; Gaussian, Inc.: Pittsburgh, PA, 1992.

(16) (a) Cradock, S.; Liescheski, P. B.; Rankin, D. W. A.; Robertson, H. E. *J. Am. Chem. Soc.* **1988**, *110*, 2758. (b) Sorensen, G. O.; Mohler, L.; Ratsup-Andersen, N. *J. J. Mol. Struct.* **1974**, *20*, 119.

(17) Breneman, C. M.; Wiberg, K. B. *J. Comput. Chem.* **1990**, *11*, 361.

(18) Carlson, H. A.; Nguyen, T. B.; Orozco, M.; Jorgensen, W. L. *J. Comput. Chem.* **1993**, *14*, 1240.

(19) Tembe, B. L.; McCammon, J. A. *Comput. Chem.* **1984**, *8*, 281.

(20) Zwanzig, R. W. *J. Chem. Phys.* **1954**, *22*, 1420.

(21) Jorgensen, W. L. *Chemtracts: Org. Chem.* **1991**, *4*, 91 and references therein.

(22) Jorgensen, W. L.; Nguyen, T. B. *Proc. Natl. Acad. Sci. U.S.A.* **1993**, *90*, 1194.

(23) Parris, K. Thesis, University of Pittsburgh, PA, 1988.

(24) Jen, M.; Lide, D. R., Jr. *J. Chem. Phys.* **1962**, *36*, 2525.

(25) Jorgensen, W. L. *BOSS*, Version 3.4; Yale University: New Haven, CT, 1993.

(26) Jorgensen, W. L.; Ravimohan, C. J. *J. Chem. Phys.* **1985**, *83*, 3050.
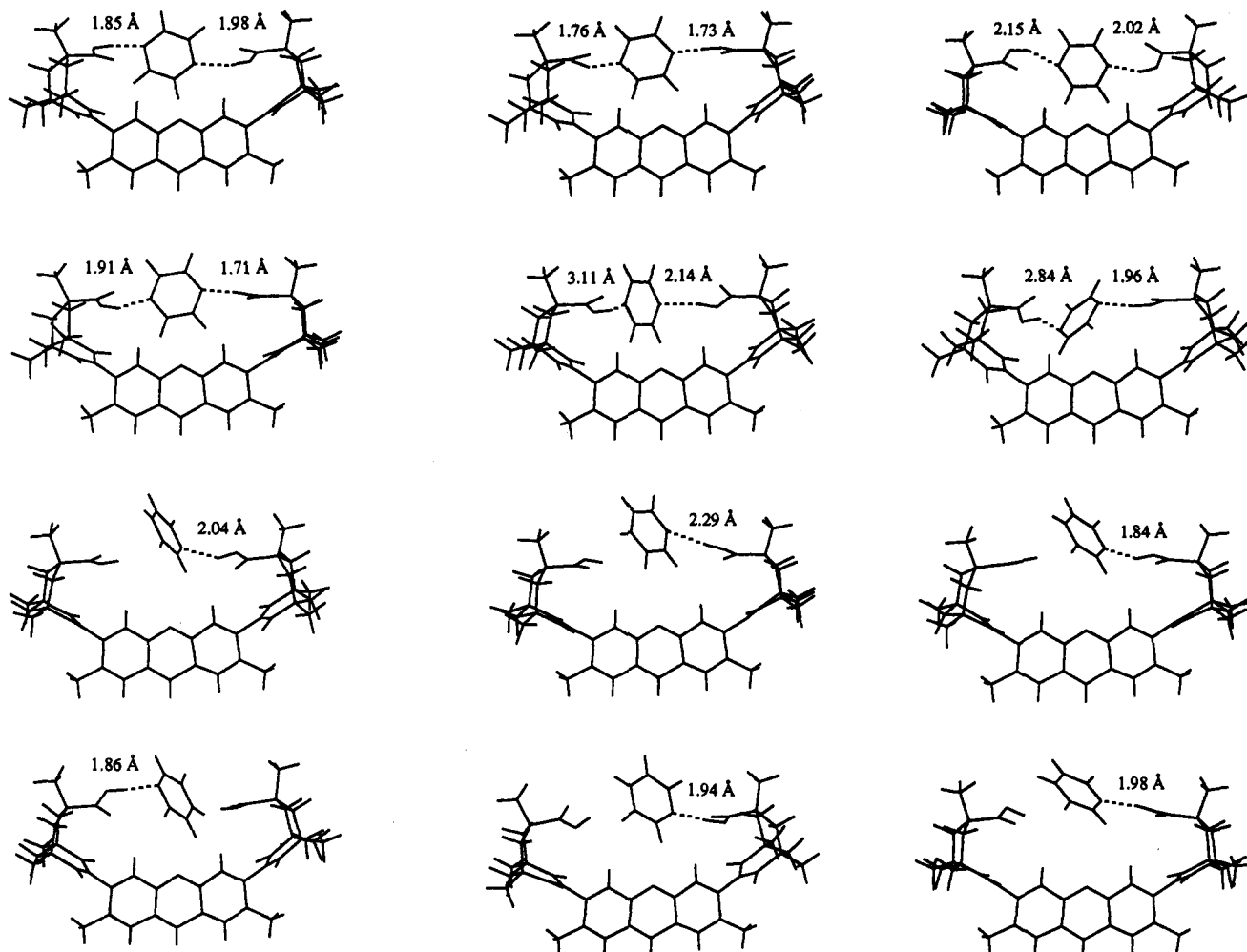
Figure 3. Random configurations from each window of the mutation from pyrazine to pyridine in the diacid host in chloroform. The mutation proceeds from left to right, top to bottom. All solvent molecules have been omitted for clarity, and acid–nitrogen hydrogen bonds have been dashed.

Notably, the complex with pyrazine (Figure 2a) exhibits symmetrical two-point binding with a net interaction energy relative to the separated host and guest of –17.17 kcal/mol. The substantial price paid to deform the host, 3.43 kcal/mol, is dwarfed by the –20.60 kcal/mol intrinsic attraction within the host–guest pair. From the picture, it appears that the pyrazine is situated in the cleft such that it takes advantage of both electrostatic interactions with the acid groups and long-range attractions to the acridine spacer. This is supported by a breakdown of the energetics of the interactions, and it may also be noted that the Coulombic and Lennard–Jones attractive terms contribute nearly equally to the net binding energies (Table 2).

The complex with pyridine, as expected, loses two-point binding (Figure 2b), and the net interaction energy rises to –13.84 kcal/mol. Although the penalty for host deformation is only 1.85 kcal/mol, the intrinsic interaction between the host–guest pair is significantly weaker at –15.69 kcal/mol. Interestingly, though it loses one hydrogen bond, the pyridine reorients itself in the cleft by flipping up to dispose the nitrogen for favorable electrostatic interactions with the distal acid group as well. This is reflected in a quantitative breakdown of the energetics, which shows that substantial long-range attractions with both the distal acid group and the acridine unit augment the one strong hydrogen bond in the host–guest interaction.

Symmetrical two-point binding is once more achieved for the complex with quinoxaline (Figure 2c). Here, the cost of deformation is the same as with pyrazine, but the intrinsic interaction is more favorable by over 6 kcal/mol, coming about equally from more attractive Coulombic and Lennard–Jones contributions. This leads to an overall optimal interaction energy

for the quinoxaline complex of –23.26 kcal/mol. The quinoxaline is aligned so that the benzenoid ring benefits from attractions to the acridine spacer, without tipping to accommodate the ideal π-stacking arrangements suggested by Rebek and co-workers.[2a] To approach the optimal distance of ca. 3.9 Å between the aromatic planes,[10] the bicyclic units would have to twist substantially about the imide–acridine junctions. However, this leads to impossibly close contacts within the host itself such as between imide oxygens and the acridine methyl groups. Nevertheless, as shown in the energetic breakdown for the fully optimized complex, the presence of the benzenoid ring strengthens all components of the interaction and especially leads to additional long-range attractions. Finally, it should be noted that both of Pascal and Ho's quinoxaline complexes, A and B in Figure 1,[4] minimize to the orientation reported here. Optimizations of the B complex with the guest fixed yield a binding energy of –16.38 kcal/mol. Though the host–guest interaction is a favorable –22.17 kcal/mol, a larger deformation fine is assessed at 5.79 kcal/mol. It therefore seems likely that the B structure reflects consequences of crystal packing rather than being a viable minimum.

Fluid Simulations. The bound mutations are depicted in "freeze-frame" style in Figures 3 and 4. In each, the solvent has been omitted for clarity. Though the structures here are snapshots from configurations near the end of each step, they are representative of the entire simulation. The free energetics, furthermore, are given in Table 3.

By following the pyrazine (Figure 3, top left) to pyridine (Figure 3, bottom right) mutation, it is clear that structures like the gas-phase minima were sampled in solution. As indicated in the individual frames, two-point binding is essentially maintained
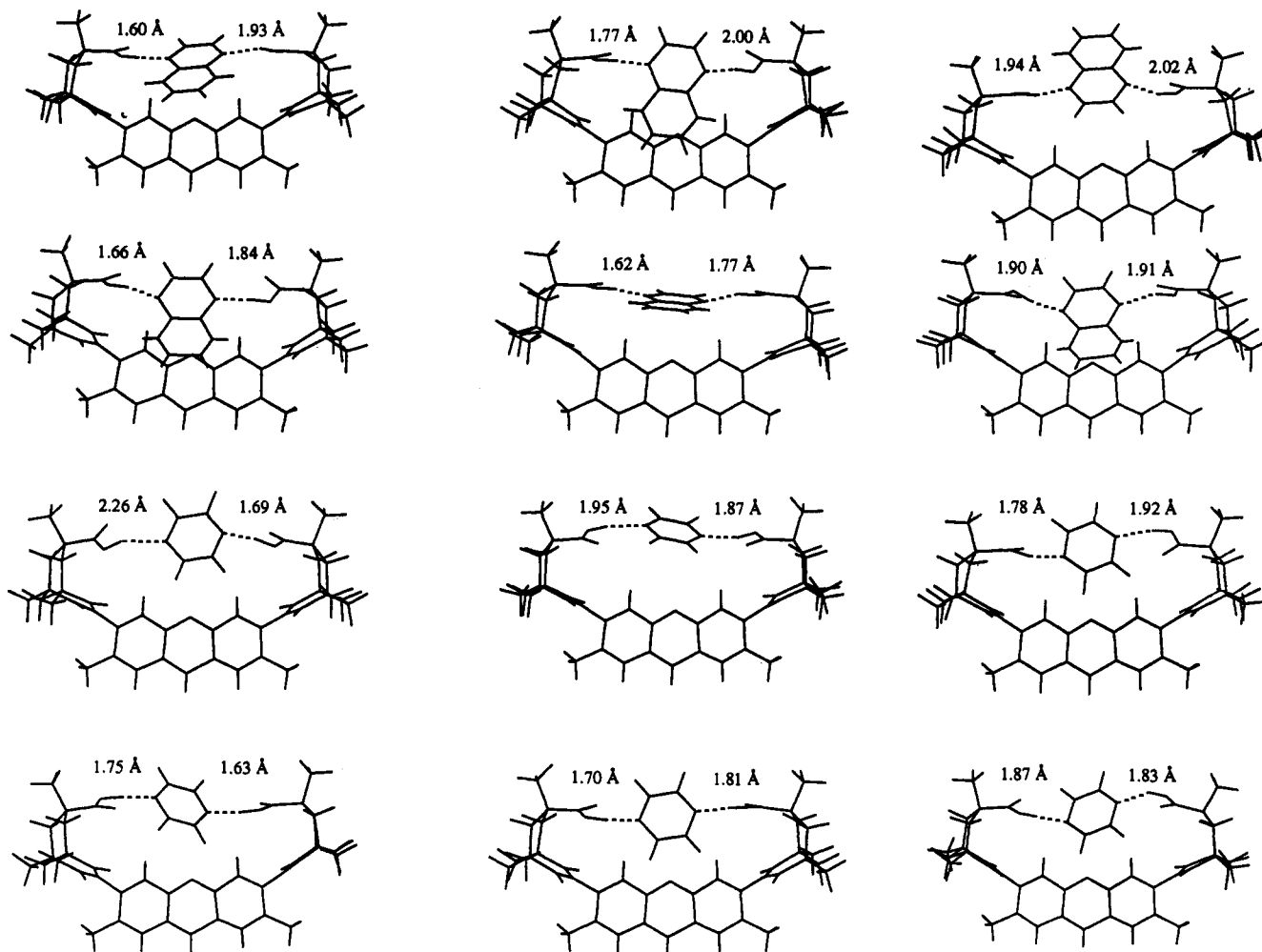
Figure 4. Progress of the mutation of quinoxaline to pyrazine bound to the diacid host in chloroform solution. Each structure corresponds to a random configuration near the end of the simulation in a particular window. Details as in Figure 3.

throughout the first half of the simulations. From that point, the guest exhibits behavior characteristic of pyridine in the gas-phase complex; it sustains one hydrogen bond to the diacid while positioning itself to profit from weaker interactions with the other acid group as well as the acridine spacer. Not surprisingly, the relative binding free energy is considerably damped from the difference in net interaction energies of the gas-phase minima. This can certainly be attributed to solvent effects as well as entropic factors associated with thermal, configurational averaging. The free energy change computed for this process favors binding pyrazine by 1.739 ± 0.106 kcal/mol (Table 3).[27] Moreover, pyrazine is marginally preferred in the unbound mutation in chloroform by 0.153 ± 0.056 kcal/mol. Combination of these results yields a relative binding free energy of 1.586 ± 0.120 kcal/mol. This translates into a K_a ratio of 14.6, which is in excellent agreement with the K_a ratio of 11.7 ($\Delta\Delta G$ = 1.45 kcal/mol) favoring pyrazine, measured by Rebek and co-workers.[2a]

By tracking the mutation of quinoxaline (Figure 4, top left) to pyrazine (Figure 4, bottom right), it is seen that the guest samples a variety of positions within the binding cleft, including ones similar to that observed in the gas-phase minimum (Figure 2c) as well as those found in the unit cell of Pascal and Ho's crystal.[4] Moreover, all of these situations preserve simultaneous two-point binding. However, as with the energy-minimized gas-phase structure, optimal π-stacking does not occur. Overall, quinoxaline is preferred in the binding pocket by 4.397 ± 0.144 kcal/mol (Table 3). The presence of the additional benzenoid ring in quinoxaline also provides for better solvation than for
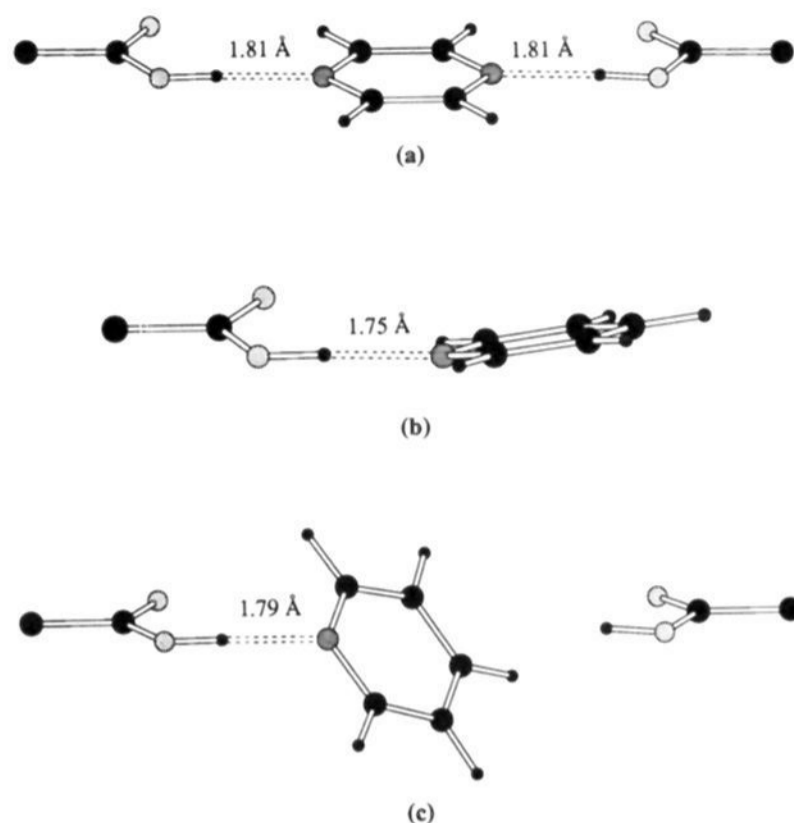
(27) The computed statistical uncertainties are ±1σ and are obtained from the fluctuations in separate averages over blocks of 2 × 10⁵ configurations.

Table 3. Incremental and Overall Free Energy Changes (kcal/mol) for the Mutations in Chloroform

λ	ΔG_λ(pyrazine → pyridine)	ΔG_λ(quinoxaline → pyrazine)
0.05	0.780 ± 0.022	0.707 ± 0.069
0.15	0.627 ± 0.041	0.496 ± 0.058
0.25	0.759 ± 0.015	0.771 ± 0.077
0.35	0.145 ± 0.060	0.640 ± 0.040
0.45	−0.068 ± 0.020	0.478 ± 0.043
0.55	−0.129 ± 0.013	0.606 ± 0.017
0.65	−0.161 ± 0.023	0.449 ± 0.023
0.75	−0.066 ± 0.023	0.186 ± 0.016
0.85	−0.178 ± 0.029	0.049 ± 0.012
0.95	0.030 ± 0.053	0.015 ± 0.044
ΔG_b	1.739 ± 0.106	4.397 ± 0.144
ΔG_u	0.153 ± 0.056	3.149 ± 0.075
$\Delta\Delta G$	1.586 ± 0.120	1.248 ± 0.162

pyrazine; the unbound mutation favors quinoxaline by a significant 3.149 ± 0.075 kcal/mol. Combination of these yields a relative free energy of binding equal to 1.248 ± 0.162 kcal/mol and a K_a ratio of 8.2, favoring quinoxaline, which can be compared with the K_a ratio of 16.4 ($\Delta\Delta G$ = 1.66 kcal/mol) observed by Rebek and co-workers.[2a] The conformational flips of the quinoxaline in the cleft during the mutation (Figure 4) are gratifying from a sampling standpoint. And, overall, the free energy results are in good accord with Rebek's binding data, including, of course, the order of binding affinities, quinoxaline > pyrazine > pyridine.

Model Studies. The optimized structures of the model complexes in the gas phase are shown in Figure 5a–c, and the relevant energetics are given in Table 4.

Figure 5. Results of gas-phase optimizations for a model diacid host with the pyrazine and pyridine guests. Parts a and c depict the energy minima of the complete diacid model cleft with pyrazine and pyridine, respectively. Part b shows the results of opimization of pyridine in the presence of a single acid group. In all, the acid–nitrogen hydrogen bonds have been dashed.
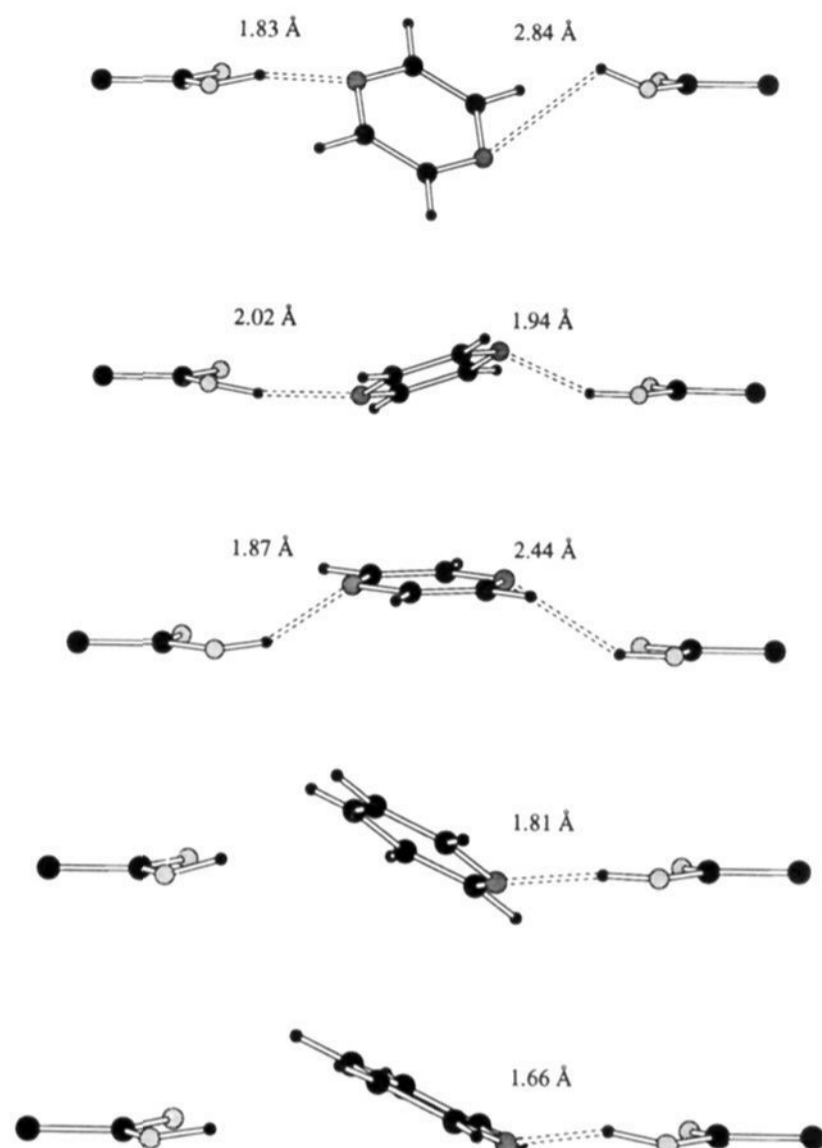
Table 4. Results of Gas-Phase Optimizations for the Model Complexes[a]

guest	model[b]	E_{XX}[c]	$1/r$	$1/r^{12}$	$1/r^6$
pyrazine	full	−14.43	−14.20	8.07	−8.30
pyridine	half	−9.73	−10.30	5.54	−4.97
pyridine	full	−12.09	−10.72	6.15	−7.52

[a] Energies in kcal/mol. [b] "Full" means both acid groups were present for the minimization; "half" indicates that only one acid group was present. [c] Model host–guest interaction energy. Its Coulombic ($1/r$) and Lennard–Jones ($1/r^{12}$ and $1/r^6$) components are also listed.

Much as expected, the fully optimized pyrazine complex (Figure 5a) has a favorable net interaction energy, near −14 kcal/mol, that is dominated by electrostatic interactions associated with the two-point binding. Meanwhile, incorporation of pyridine in the model cleft affords interesting results (Figure 5b,c). Removing the distant acid group results in a penalty of nearly 5 kcal/mol on the pyrazine net interaction energy, with comparable loses in all components of the interaction. However, optimizations in the presence of both acids recover nearly 2.5 kcal/mol of that energy, mostly in the attractive Lennard–Jones interactions.[28] The structure of this complex (Figure 5c) is reminiscent of the pyridine–diacid complexes both in the gas-phase minimum and throughout the final steps of the mutation in chloroform; pyridine establishes itself to enjoy both one strong hydrogen bond with the proximal acid group and a distribution of weaker interactions with the distal acid functionality.

The mutation of pyrazine to pyridine in the model cleft in chloroform evolved in a manner similar to the mutation in the acridine diacid, as can been visualized in Figure 6. Specifically, two-point binding is upheld throughout the first half of the mutation, and later steps produce pyridine-like binding patterns. Quantitatively, pyrazine is preferred by 2.067 ± 0.116 kcal/mol in this model mutation. Combination of that result with the ΔG_u reported above gives a relative binding free energy of nearly 1.9 kcal/mol and a resultant K_a ratio of 25.3, favoring pyrazine. Overall, these results are quite similar to those obtained for the actual host–guest system. In fact, many of the molecular

---

(28) The separation of the two acids was fixed at the optimal value for the pyrazine complex (Figure 5a).


Figure 6. Random configurations of the model pyrazine to pyridine mutation in chloroform. The simulation proceeds from top to bottom, and details are as in Figures 3 and 4.

recognition aspects of the problem appear to be reflected in the interactions observed in the model system.

Comparison with Earlier Results. Clearly, it was important in both the initial computational study and this investigation to understand the origin of the modest K_a ratio that favored pyrazine over pyridine binding to the diacid. Afterall, it seemed surprising that the loss of a hydrogen bond upon mutation to pyridine amounted to a mere 1.5 kcal/mol. In the reverse sense, having paid the entropic price to engineer one hydrogen bond in the solvated cleft, making the second hydrogen bond should be facile and energetically profitable. Given the accuracy with which the initial computational study reproduced the K_a ratio,[3] it appeared resonable that the small difference arose from the inability of the acridine diacid to hold the pyrazine in a simultaneous two-point binding fashion. In this way, the preferential binding of pyrazine resulted from additional weak interactions between the uninvolved acid–nitrogen couple. What is demonstrated here, however, is that the formal loss of one hydrogen bond upon mutation to pyridine is in a large sense compensated by significant interactions with the distant acid group and, in fact, the entire framework. As such, the relative binding free energy is smaller than might be expected.

The structural disagreement between the initial and present computational studies was also probed. To this end, relevant acridine diacid structures were examined, with the key parameter being the distance between the singly-bonded oxygen atoms of the acid groups that defined the binding cleft. These are shown in Figure 7. As a frame of reference, the original Rebek diacid that was crystallized as the monomethyl ester (Figure 7a) had an O_{Me}–O_H distance of 7.84 Å.[23] When pyrazine was introduced into the binding pocket, as demonstrated in the unpublished Pascal and Ho structure at 235 K (Figure 7b), the separation widened to 8.25 Å.[5] Moreover, full optimization using the present all-atom force field of the diacid with pyrazine in the cleft yielded
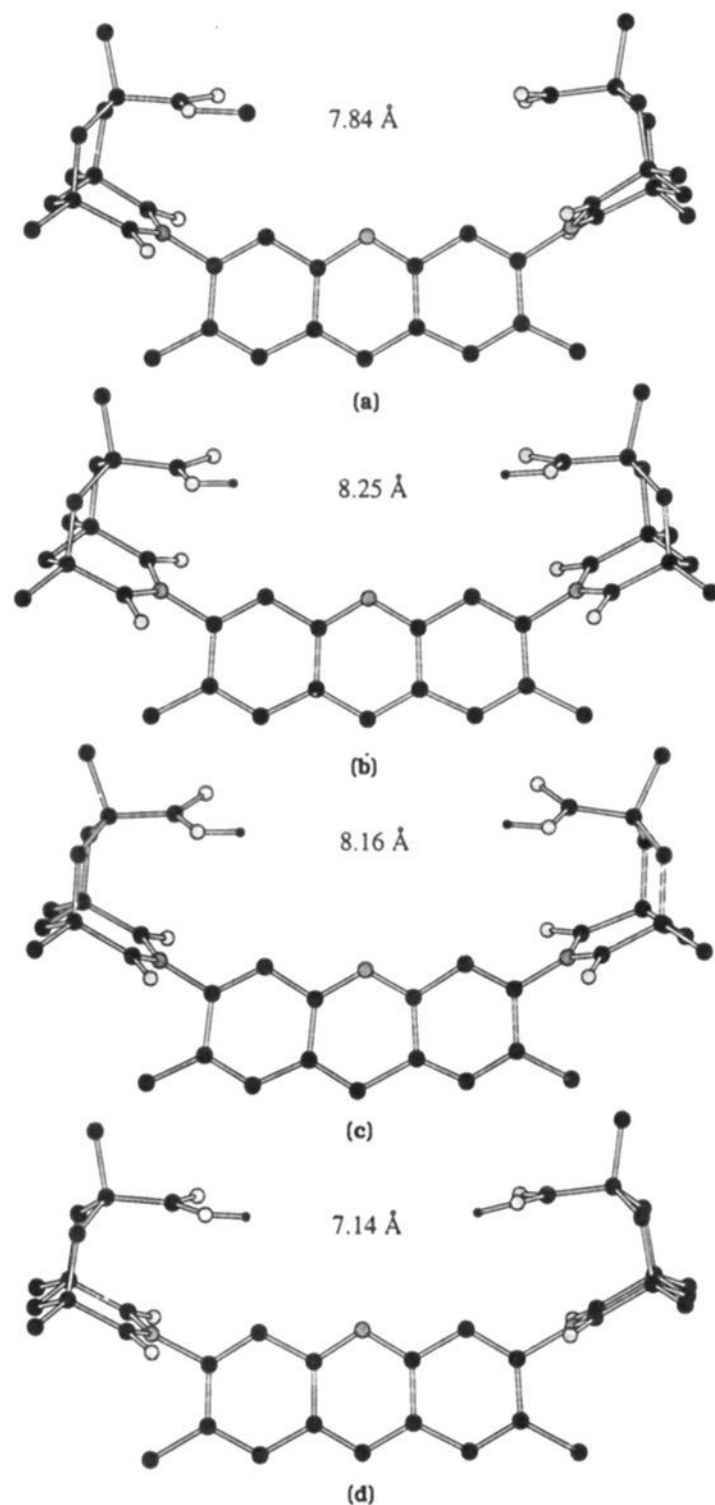
Figure 7. Selected host structures for comparison of cleft size. Nonpolar hydrogens are not shown. Where necessary, guest molecules are stripped from the host for clarity. The distance between the O_H–O_H atoms in the opposing acid groups is displayed. (a) Original Rebek diacid, as the monomethyl ester. (b) Unpublished Pascal and Ho structure at 235 K of the host after complexation with pyrazine. (c) Host, after full optimization with pyrazine in the binding pocket, used in this study. (d) Host, after constrained optimization of an MM2 structure with pyrazine, used in the initial computational investigation.

a similar O_H–O_H distance of 8.16 Å (Figure 7c). Yet, the host used in the earlier simulations, which was the result of constrained optimization of an MM2 structure and pyrazine (Figure 7d), had a narrower cleft at 7.14 Å.[3] Apparently, the nearly 1-Å contraction in the cleft was enough to deny true two-point binding of pyrazine. Furthermore, there is no question that inclusion of complete flexibility in the bicyclic regions and employment of the more sophisticated all-atom force field yielded structural and energetic results that are fully consistent with experiment.

Mulliken Charges. The host–guest interactions described here are expected to be sensitive to the model chosen to represent the electrostatics in the guest molecules. However, gas-phase optimizations of the diacid and its pyrazine and pyridine complexes employing the 6-31G(d) Mulliken charges for the guests afford net interaction energies and structures that are very similar to those found with the CHELPG charge set (Table 1). Though the host–guest intrinsic interactions are more attractive at –25.24 and –20.07 kcal/mol for pyrazine and pyridine, respectively, the deformation penalties are greater as well such that the difference in net interaction energies is also on the order of 3 kcal/mol, favoring pyrazine. Interestingly, the fluid mutations performed with the Mulliken charges for pyrazine and pyridine exhibited the same behavior of the guests in the binding cleft and nearly identical energetics. In particular, the computed ΔG_b favors pyrazine by 1.668 ± 0.109 kcal/mol and pyrazine is slightly better solvated than pyridine by 0.081 ± 0.062 kcal/mol. Overall, then, the relative free energy of binding falls in favor of pyrazine by 1.587 ± 0.125 kcal/mol for a K_a ratio of 14.6, which is identical to the results with the CHELPG charges.

Conclusion

The present study has brought the modeling of the host–guest chemistry for binding with Rebek's acridine diacid up to current standards. Utilization of an all-atom force field introduces adequate flexibility into the host to allow the two-point binding of diazenes, which has recently been supported by X-ray crystallography. The results of the free energy calculations further support the structural findings through good reproduction of the quantitative experimental data on binding.

Supplementary Material Available: A listing of the OPLS nonbonded and torsion parameters for the host–guest systems (3 pages) is available. This material is contained in many libraries on microfiche, immediately follows this article in the microfilm version of the journal, and can be ordered from the ACS; see any current masthead page for ordering information.